

LISA source confusion

Jeff Crowder and Neil J. Cornish

Department of Physics, Montana State University, Bozeman, Montana 59717, USA

(Received 3 May 2004; published 27 October 2004)

The Laser Interferometer Space Antenna will detect thousands of gravitational wave sources. Many of these sources will be overlapping in the sense that their signals will have a nonzero cross correlation. Such overlaps lead to source confusion, which adversely affects how well we can extract information about the individual sources. Here we study how source confusion impacts parameter estimation for galactic compact binaries, with emphasis on the effects of the number of overlapping sources, the time of observation, the gravitational wave frequencies of the sources, and the degree of the signal correlations. Our main findings are that the parameter resolution decays exponentially with the number of overlapping sources and superexponentially with the degree of cross correlation. We also find that an extended mission lifetime is key to disentangling the source confusion as the parameter resolution for overlapping sources improves much faster than the usual square root of the observation time.

DOI: 10.1103/PhysRevD.70.082004

PACS numbers: 95.55.Ym, 04.80.Nn, 95.85.Sz

I. INTRODUCTION

It is anticipated that the Laser Interferometer Space Antenna (LISA) [1] will start collecting data in the next decade. LISA will operate in the source-rich low frequency portion of the gravitational wave spectrum, where the primary sources are expected to be compact galactic binaries, supermassive black hole binaries, and extreme mass ratio inspirals (such as a white dwarf falling into a supermassive black hole). A natural question to ask is how well the source parameters, such as sky location, masses, and distances, can be recovered from the LISA data stream. Estimates of the parameter resolution have been given for compact galactic binaries [2–4], supermassive black hole binaries [2,3,5–7], and extreme mass ratio inspirals [8]. These studies focused on the problem of identifying one source at a time and did not address the problem of source confusion. The large signal from the galactic population of close white dwarf binaries was not ignored, but it was treated as an additional source of stationary, Gaussian noise to be added to the instrument noise. We will see that this is not a good approximation.

Here we study how parameter estimation is affected by the presence of multiple overlapping signals in the LISA data stream. Importantly, we find that the behavior is very different from what one would predict by treating the additional sources as stationary, Gaussian noise. The problem of source confusion will be most pronounced below ~ 2 mHz, where it is expected that many tens to tens of thousands of galactic binaries will have signals that overlap in each frequency bin [9]. Thus, we will focus our attention on low frequency galactic binaries that are close to one another in frequency. This work uses only optimal signal processing, in which one solves for the parameters of all sources simultaneously. Suboptimal signal processing, solving for the parameters of one source while other sources are disregarded or treated as an effective noise, is not addressed by this work.

The paper is organized as follows: We begin with a summary of our findings in Sec. II. This is followed by a review of parameter estimation for an isolated galactic binary in Sec. III. Parameter estimation with multiple sources is described in Sec. IV, and our plan for exploring the parameter space is described in Sec. V. The main results are described in Sec. VI. A brief information theory perspective is presented in Sec. VII, and concluding remarks are made in Sec. VIII.

II. SUMMARY OF RESULTS

We find that the parameter estimation uncertainties grow exponentially with the number N of overlapping sources. This should be contrasted to the \sqrt{N} increase one would predict if the other sources were treated as stationary, Gaussian noise. The degradation in resolution was found to be nearly uniform across the seven parameters that LISA will measure for a galactic binary system. As one might expect, the parameter uncertainties are a strong function of the signal cross correlations. We find that as the two signals become more correlated, the parameter estimation uncertainties grow at a rate that is faster than exponential. Importantly, we find that the parameter uncertainties decrease rapidly as the observation time T is increased—far more rapidly than the usual $1/\sqrt{T}$ improvement one expects when competing with stationary, Gaussian noise.

III. REVIEW OF PARAMETER ESTIMATION

Typical galactic binaries can be treated as circular and monochromatic. They are described by seven parameters: sky location (θ, ϕ) ; gravitational wave frequency f ; amplitude A ; inclination and polarization angles (ι, ψ) ; and the initial orbital phase γ . The response of the LISA instrument to a gravitational wave source is encoded in the (Micheleson-like) $X(t)$ and $Y(t)$ time-delay interfer-

ometry variables [10]. We employ the rigid adiabatic approximation [11] to describe these variables and work with the orthogonal combinations [2]

$$S_I(t) = X(t), \quad S_{II}(t) = \frac{1}{\sqrt{3}}[X(t) + 2Y(t)]. \quad (1)$$

Each signal is a function of the parameters $\vec{\lambda} \rightarrow (\theta, \phi, f, A, \iota, \psi, \gamma)$ that describe the source. Denoting the one-sided noise spectral power by $S_n(f)$, we adopt the usual noise-weighted inner product

$$\langle a|b \rangle = 2 \int_0^\infty \frac{a^*(f)b(f) + a(f)b^*(f)}{S_n(f)} df. \quad (2)$$

Decomposing the output channels into signal h and noise n , the signal-to-noise ratio (SNR) is given by

$$\text{SNR}^2 = \sum_{\alpha=I,II} \langle h_\alpha | h_\alpha \rangle. \quad (3)$$

For large SNR the parameter estimation uncertainties $\Delta\lambda^i$ will have the Gaussian probability distribution [12]

$$p(\Delta\lambda^i) = \sqrt{\frac{\det(\Gamma)}{2\pi}} \exp\left(-\frac{1}{2} \Gamma_{ij} \Delta\lambda^i \Delta\lambda^j\right), \quad (4)$$

where the Fisher information matrix Γ is defined by

$$\Gamma_{ij} = \sum_{\alpha=I,II} \langle h_{\alpha,i} | h_{\alpha,j} \rangle. \quad (5)$$

Here $h_{\alpha,i} = \partial h / \partial \lambda^i$. For large SNR the variance-covariance matrix is given by

$$C^{ij} = (\Gamma^{-1})^{ij}, \quad (6)$$

and the uncertainties in the parameters are given by $\Delta\lambda^i = (C^{ii})^{1/2}$. The volume of the $n - \sigma$ uncertainty ellipsoid in the d dimensional parameter space is

$$V_d = \frac{\pi^{d/2} n^d}{\Gamma(d/2 + 1)} \sqrt{\det C_{ij}}. \quad (7)$$

Applying the above formalism to an isolated galactic $0.5 M_\odot$ white dwarf binary yields the parameter uncertainties shown in Figs. 1 and 2. The plots were generated by taking the median values for 10^5 different sources, each normalized to a 1 yr signal-to-noise ratio of $\text{SNR} = 10$. The uncertainty in the frequency has been increased by a factor of 10^6 for plotting purposes. Note: While almost all white dwarf binaries have frequencies below 5 mHz Fig. 1 and 14 extend out to 10 mHz to emphasize the trends that are occurring.

As can be seen in Fig. 1, the uncertainties in five of the seven parameters are fairly constant across the LISA band. The two exceptions are the sky location variables (θ, ϕ), which show a marked decrease in their uncertainties above 1 mHz. This behavior can be traced to the time varying Doppler shift, which is one of the two ways LISA is able to locate sources on the sky. The Doppler shift

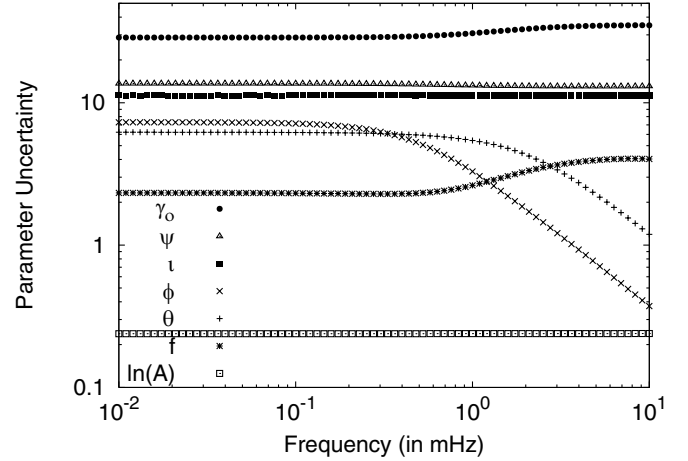


FIG. 1. Median parameter uncertainties versus frequency for isolated monochromatic binary sources with 1 yr of observation and fixed signal-to-noise ratios of $\text{SNR} = 10$. The parameters are $f, \ln A, \theta, \phi, \iota, \psi, \gamma$.

increases linearly with f , which translates into a $1/f$ decrease in the positional uncertainties above 1 mHz. Below this frequency the angular resolution comes mainly from the time varying antenna sweep, which is weakly dependent on f below the transfer frequency $f_* \approx 10$ mHz.

As can be seen in Fig. 2, the uncertainties in six of the seven parameters decrease as $1/\sqrt{T_{\text{obs}}}$ for observation times longer than a year, in accordance with the standard $\sqrt{T_{\text{obs}}}$ increase in the SNR. The one exception is the frequency, which benefits from an additional $1/T_{\text{obs}}$ shrinkage in the width of the frequency bins, leading to an overall $1/T_{\text{obs}}^{3/2}$ decay in the frequency uncertainty. The shrinkage in the size of the frequency bins is illustrated in

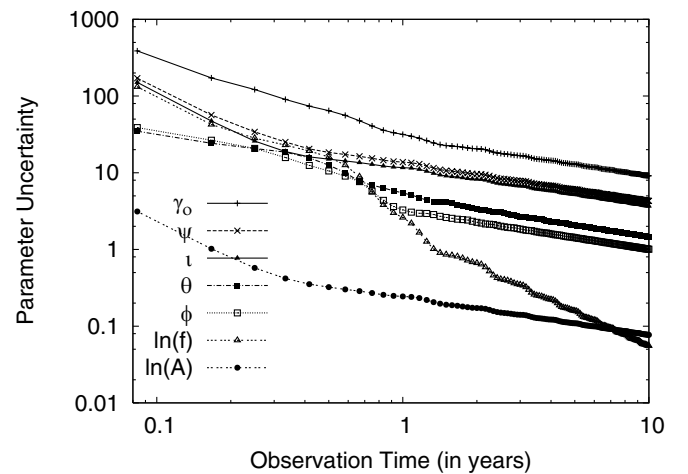


FIG. 2. Parameter uncertainties versus time for isolated monochromatic binary sources with $f = 1$ mHz and signal-to-noise ratios normalized to $\text{SNR} = 10$ for 1 yr of observation. The parameters are $\ln f, \ln A, \theta, \phi, \iota, \psi, \gamma$.

Fig. 3, where the power spectrum of a typical source is shown after 1 yr and after 10 yr of observation. Later we will see how this improved resolution of the sidebands helps reduce source confusion when multiple overlapping sources are present.

In what follows, we will typically quote our results in terms of uncertainty ratios. These ratios will compare the parameter resolution when one or more overlapping sources are present to the parameter resolution that would be possible if each source were isolated. To arrive at the absolute uncertainties one needs to multiply by the isolated source uncertainties quoted above.

IV. MULTIPLE SOURCES

The Fisher information matrix approach to estimating parameter uncertainties is easily generalized to multiple sources. For N circular, monochromatic binary systems, the parameter space is $7N$ dimensional, and we have the

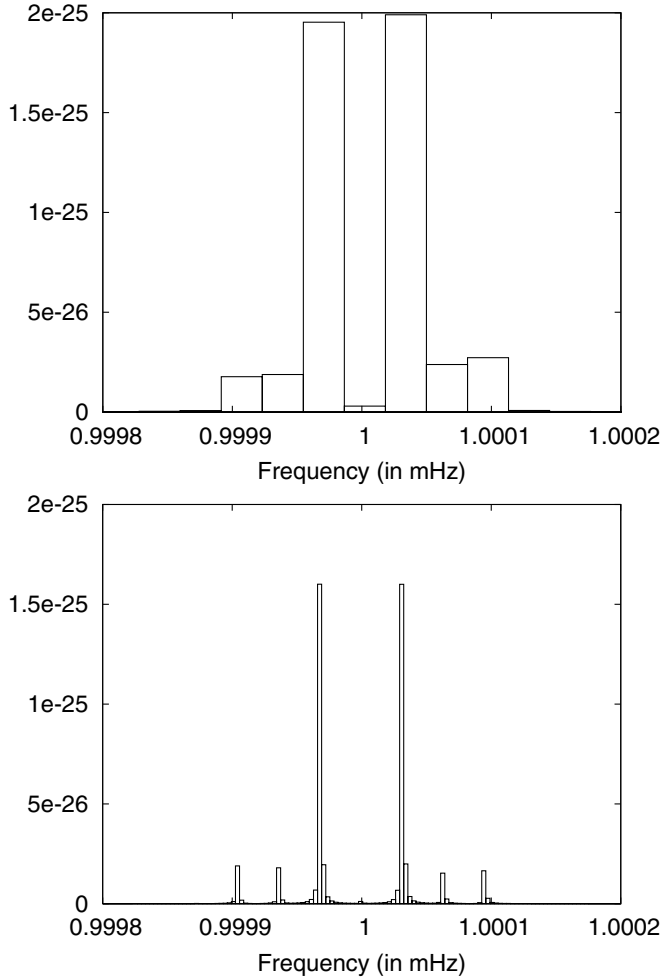


FIG. 3. Power spectrum of a $0.5 M_{\odot}$ 1 mHz white dwarf binary for observation times of 1 and 10 yr. Source parameters: $\theta = 1.60$, $\phi = 3.50$, $f = 1.00$ mHz, $A = 1.49 \times 10^{-22}$, $\iota = 0.489$, $\psi = 0.357$, $\gamma_o = 3.527$.

parameter vector

$$\vec{\Lambda} = \vec{\lambda}^1 + \vec{\lambda}^2 + \dots + \vec{\lambda}^N. \quad (8)$$

We will use the notation Λ^A to refer to all seven parameters of the A^{th} binary. The total signal $S = S_I$ or $S = S_{II}$ will be the sum of the signals for the individual binary systems,

$$S = S^1 + S^2 + S^3 \dots + S^N. \quad (9)$$

Here S^A is the signal due to the A^{th} binary. Since $\partial S^A / \partial \Lambda_B = 0$ for $A \neq B$, the full Fisher information matrix has a simple structure. If we define

$$\Gamma_{AB} = \sum_{\alpha=I,II} \left\langle \frac{\partial S^A_{\alpha}}{\partial \Lambda_A} \middle| \frac{\partial S^B_{\alpha}}{\partial \Lambda_B} \right\rangle, \quad (10)$$

the diagonal blocks Γ_{AA} are the usual 7×7 Fisher information matrix for the A^{th} source, while the off-diagonal blocks Γ_{AB} describe how the parameter estimation for source A is influenced by the presence of source B and vice versa. If all the sources are uncorrelated (for example, they might be widely spaced in frequency), then the off-diagonal blocks will be zero, and the full Fisher information matrix will be block diagonal. Upon inverting to get the variance-covariance matrix the block diagonal structure will be preserved, with each 7×7 block equal to the inverse of the corresponding single source Fisher information matrix. However, if the sources are overlapping, the off-diagonal blocks will be nonzero, which will affect the values of the diagonal elements in the full variance-covariance matrix. The number of off-diagonal elements grows quadratically with the number of sources, while the number of diagonal elements grows linearly with the number of sources. Thus, we anticipate that the ability to resolve a particular source's parameters will degrade rapidly as the number of correlated sources increases.

We also anticipate that the parameter uncertainties will depend strongly on the degree of correlation between sources. The correlation between two signals S^A and S^B is defined

$$\kappa_{AB} = \frac{\langle S^A | S^B \rangle}{\langle S^A | S^A \rangle^{1/2} \langle S^B | S^B \rangle^{1/2}}. \quad (11)$$

In analyzing the results, two similar approaches will be used to obtain a quantitative measure of the increase in the parameter estimation uncertainties. First is a global comparison of the uncertainties. The uncertainties form an ellipsoid in the parameter space whose volume is given by the determinant of the variance-covariance matrix. One measure of the uncertainty increase due to the correlation of the binary systems is given by a ratio of the geometric mean of the uncertainties (GMUR):

$$\text{GMUR} \equiv \left(\frac{\det \Gamma}{\prod_A \det \Gamma_{AA}} \right)^{1/7N}. \quad (12)$$

The GMUR describes the mean increase in the parameter uncertainties due to source confusion.

A second measure of the uncertainty increase is a parameter by parameter comparison, looking at the ratio of the parameter uncertainty (PUR) between the uncertainty of a particular parameter calculated in the $7N$ -dimensional variance-covariance matrix, $\Delta \Lambda_x^A$, and the uncertainty of the same parameter calculated in the isolated binary's variance-covariance matrix, $\Delta \lambda_x^A$,

$$\text{PUR}^i \equiv \frac{\Delta \Lambda_x^i}{\Delta \lambda_x^i}. \quad (13)$$

This definition for the PUR is independent of the amplitudes of the sources, as can be seen in the simple case of two sources, each described by one α . The PUR for α_1 is given by

$$\text{PUR}_{\alpha_1} = \frac{\Delta \Lambda_{\alpha_1}}{\Delta \lambda_{\alpha_1}} = \frac{1}{\sqrt{1 - \Sigma_{\alpha_1 \alpha_2}^2}}, \quad (14)$$

where

$$\Sigma_{\alpha_1 \alpha_2} \equiv \frac{\Gamma_{\alpha_1 \alpha_2}}{\sqrt{\Gamma_{\alpha_1 \alpha_1} \Gamma_{\alpha_2 \alpha_2}}}. \quad (15)$$

The independence of the degree of confusion on the source amplitudes would seem to imply that an arbitrarily weak source can affect parameter estimation to the same degree as an arbitrarily strong source. Clearly, this makes no sense in the limit that the amplitude of the weak source goes to zero. The resolution to this apparent paradox is that the Fisher information matrix approach is only meaningful for sources with $\text{SNR} > 1$, so arbitrarily weak sources are not permitted in the analysis.

V. SOURCE PARAMETER SELECTION

The parameter space for N slowly evolving binaries is $7N$ dimensional. This large dimensionality makes it difficult to carry out an exhaustive exploration of all the circumstances that can affect parameter estimation. We focused on sources that were close in frequency and chose the other source parameters randomly. The frequency chosen for the first binary fixes the base frequency f_{base} of a data run. The frequencies of the remaining $N - 1$ binaries were assigned frequencies of $f_{\text{base}} + (i + x)f_m$, where $f_m = 1/\text{yr}$ is the modulation frequency, i is an integer, and x is a random number between 0 and 1. Thus the remaining binaries are between i and $i + 1$ modulation frequency units from the base frequency. Sky locations were chosen by two methods, the first being a random draw on $\cos(\theta) \in [-1, 1]$ and $\phi \in [0, 2\pi)$ with

a fixed distance to the binary of 1 kpc, the second being a random draw from a galactic distribution [9] of θ , ϕ , and binary distance. The values of the polarization ψ and orbital phase γ_o were randomly drawn between 0 and π and 0 and 2π respectively. The inclination ι was taken from a random draw on $\cos(\iota) \in [-1, 1]$ but with values outside of the range $\iota \in [1^\circ, 179^\circ]$ rejected to avoid the degeneracy in the gravitational wave produced by a circular binary viewed along its axis. Masses were taken to equal $0.5 M_\odot$, as we wished to model white dwarf binaries.

The signal-to-noise ratios for the sources, while not affecting the uncertainty ratios, may be of interest. Almost all ($99.98^+\%$) sources drawn from an all-sky random draw, at 1 mHz with the 1 kpc fixed distance, had signal-to-noise ratios above ten at 1 yr of observation. Figure 4 shows the signal-to-noise ratio for 99.8% of 10^6 sources from a galactic draw. The differences in the signal-to-noise ratios between the two distributions is due to the different source distances, as well as the location of the galactic disc with respect to LISA's antenna patterns. While there are some sources with signal-to-noise ratios below one, this ends up not affecting the results which are independent of source amplitude (i.e., both can be scaled up or chosen again from the distribution).

VI. RESULTS

A. Varying time of observation

The current lifespan of LISA is estimated to be 5 yr. Our data show that the longer LISA observes the binaries systems, the less the effect of confusion between sources. Figure 5 shows the median parameter uncertainty ratios for two, three, and four binary systems with base fre-

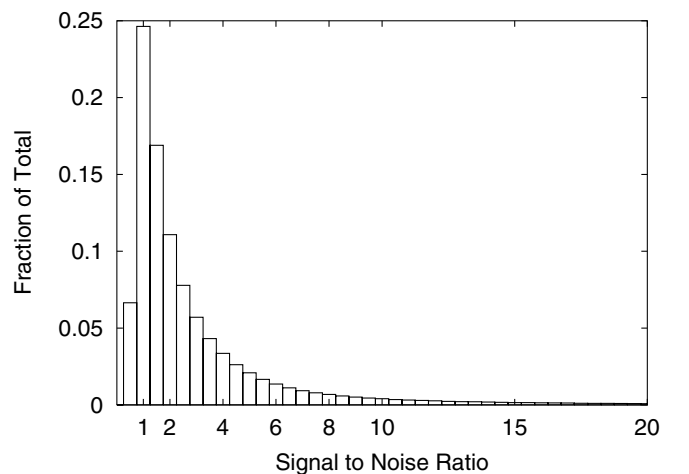


FIG. 4. Histogram of the signal-to-noise ratio for 10^6 $0.5 M_\odot$ galactic white dwarf binary sources at 1 mHz for 1 yr of observation. More than 99.8% of the sources are shown in the plot.

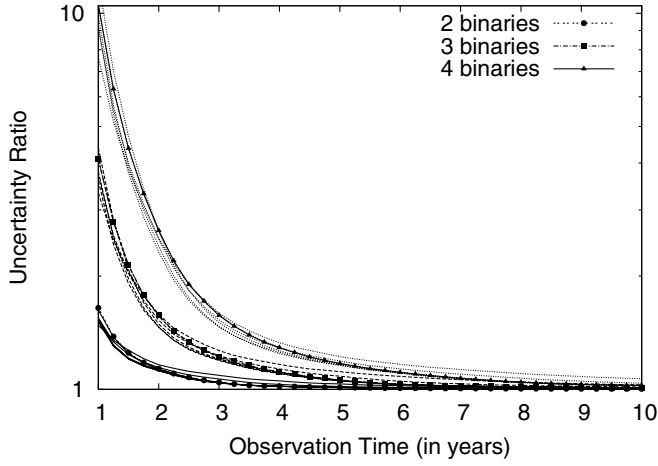


FIG. 5. Median values of the seven PURs versus time of observation for two, three, and four binaries with base frequencies of 1 mHz from an all-sky draw of 10^5 sets of sources. This demonstrates the marked, desirable decrease in the source confusion as the time of observation is extended, as well as the uniformity of confusion across all seven parameters.

quencies of 1 mHz as a function of the time of observation. Figure 6 shows the median geometric mean uncertainty ratio for the same data. Each set of PUR data in Fig. 5 contains the uncertainty ratios for all seven parameters, and as can be seen in the figures, the uncertainty ratios for each of the seven parameters are closely related. This relationship holds true for other frequencies in the LISA band. It is this level of uniformity in the increase in parameter uncertainties that motivates our use of the GMUR as an estimate for the individual PURs. Thus, subsequent results will be given in terms of the GMUR.

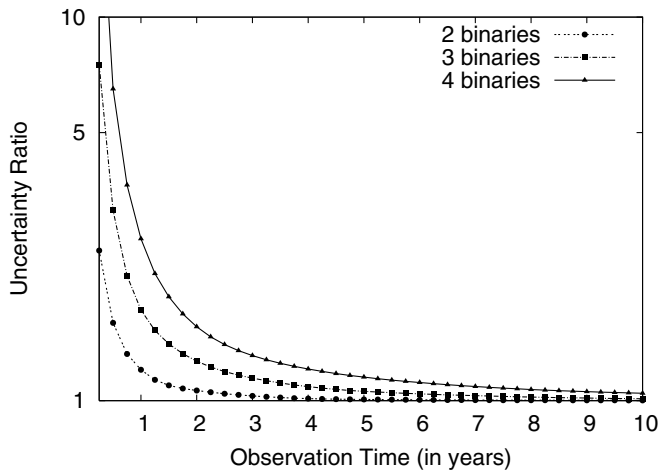


FIG. 6. Median GMUR versus time of observation for two, three, and four binaries with base frequencies of 1 mHz from an all-sky draw of 10^5 sets of sources. Again demonstrating the large decrease in the source confusion as the time of observation is extended.

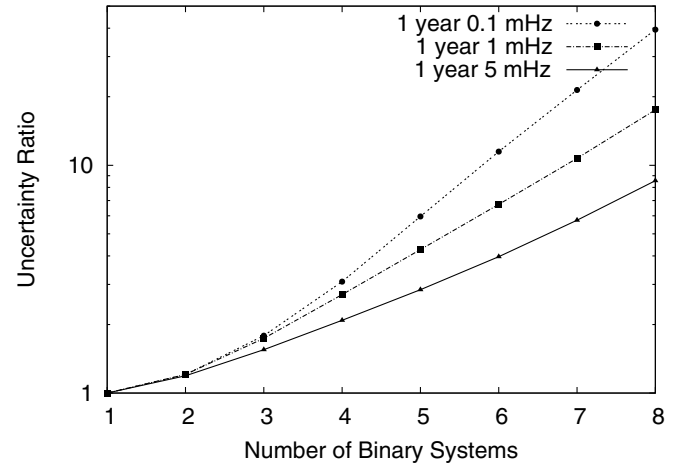


FIG. 7. Median GMUR plotted against the number of binary systems for 1 yr of observation at base frequencies of 0.1, 1, and 5 mHz from all-sky draws of 10^5 pairs of sources each. With the increase in source frequency comes an increased Doppler shift and a corresponding decrease in source confusion.

Figure 7 shows how the median GMUR increases with the number of binaries for 1 yr of observation, at base frequencies of 0.1, 1, and 5 mHz. One can see that as the Doppler shift begins to become more of a factor, source confusion is correspondingly decreased (see Sec. VI D for more detail on the effect of Doppler shifts). Figure 8 shows how extending the time of observation affects the GMUR. In both instances, the parameter uncertainties increase roughly exponentially with the number of overlapping sources.

Figure 9 shows the median of the magnitude of the correlation between the signals of two binary systems

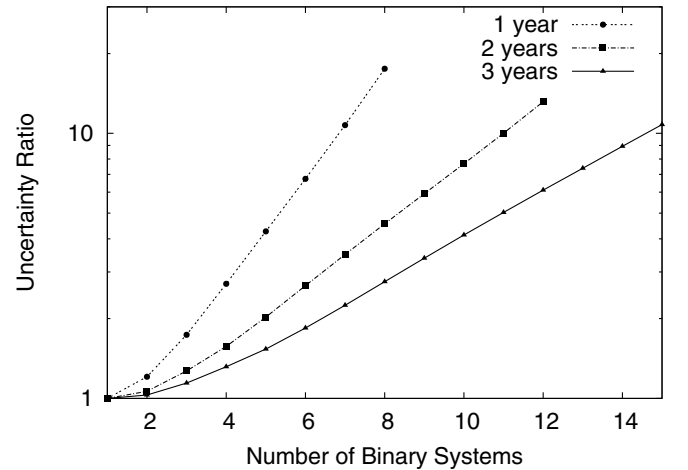


FIG. 8. Median GMUR plotted against the number of binary systems for one, two, and three years of observation at a base frequency of 1 mHz from an all-sky draw of 10^5 pairs of sources. This displays both the nature of the increase in confusion as more sources are added and the decrease in confusion as the time of observation is extended.

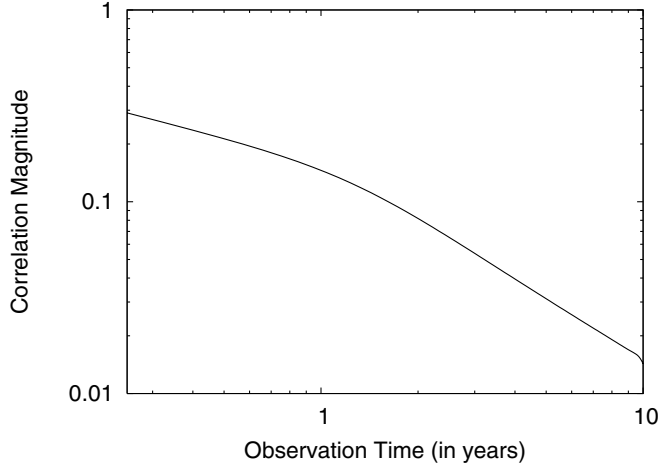


FIG. 9. Median signal correlation magnitude versus time of observation for two binaries with a base frequency of 1 mHz from an all-sky draw of 10^5 pairs of sources. One can see the correlation falling off as $1/T_{\text{obs}}$ for $T_{\text{obs}} > 1$ yr as predicted by (11).

with a base frequency of 1 mHz taken from an all-sky draw. As expected, the correlation magnitude falls off as $1/T_{\text{obs}}$ for observation times greater than a year (the numerator in (11) oscillates, while the denominator grows as T_{obs}). The $1/T_{\text{obs}}$ falloff in the signal correlation should be contrasted with the much faster falloff in the GMUR seen in Fig. 8. The reason for this difference in falloff will become clear in Sec. VIC.

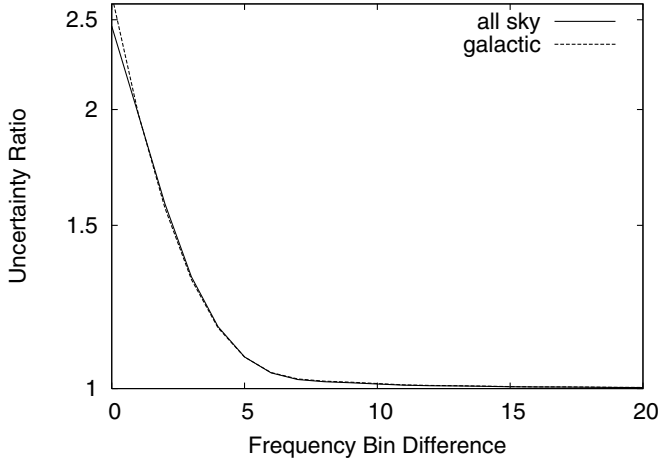


FIG. 10. Median GMUR plotted against modulation frequency bin difference of two binaries from an all-sky and a galactic draw with a base frequency of 1 mHz and 1 yr of observation for galactic and all-sky draws of 10^5 pairs of sources each. The marked falloff is due to the decreasing overlap in the source signals, making it much easier to differentiate sources separated in frequency.

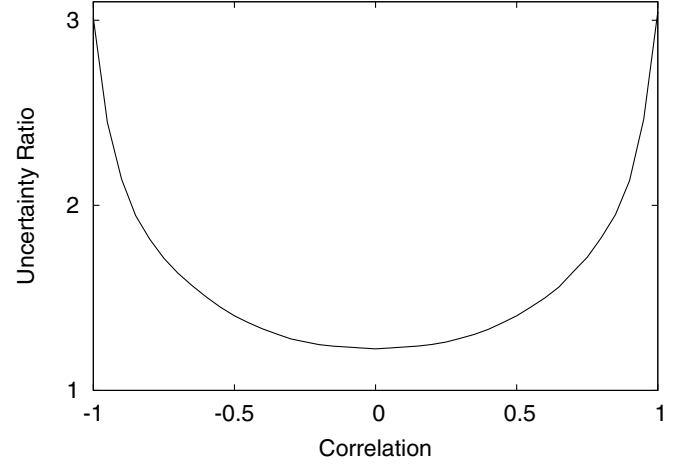


FIG. 11. The median GMUR plotted against signal correlation of two binaries from a galactic draw with a base frequency of 1 mHz and 1 yr of observation of 10^6 pairs of sources. This rapid decrease in GMUR with a decrease in correlation magnitude combines with the correlation decreases seen in Fig. 9 to create the large effects seen in Fig. 6 as the time of observation is extended.

B. Uncertainty ratios for two binary systems as a function of frequency difference

Figure 10 shows how the median parameter uncertainties depend on the frequency separation when two binary systems are present. The base frequency f_{base} for the first binary was held fixed at 1 mHz, while the frequency of the second binary was randomly chosen between $f_{\text{base}} + if_m$ and $f_{\text{base}} + (i+1)f_m$ for i between 0 and 20. Figure 10 shows the plots for GMUR versus i for all-sky and galactic draws for 1 yr of observation.

The uncertainty ratio drops rapidly as the frequency separation increases, approaching unity by the time the binaries are $\sim 5f_m$ apart. The frequency difference of

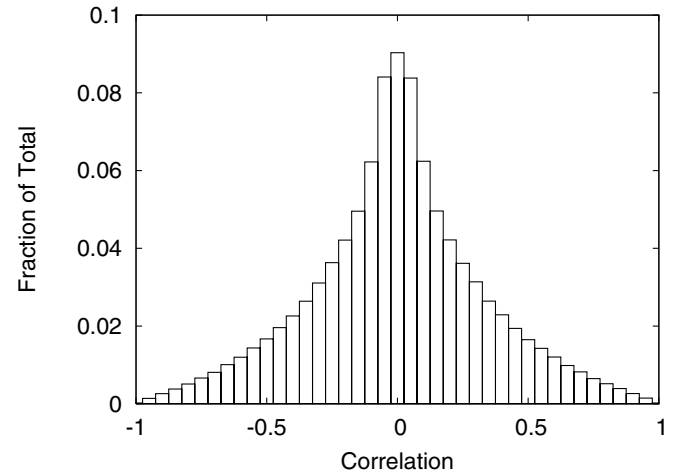


FIG. 12. A histogram of the correlation of two binaries from a galactic draw with a base frequency of 1 mHz and 1 yr of observation of 10^6 pairs of sources within $1f_m$ of each other.

$\sim 5f_m$ corresponds to the typical half-bandwidth of a source at 1 mHz. In other words, 1 mHz sources separated by $>5f_m$ have almost no overlap, and thus there is little source confusion for $i > 5$.

This result also sheds more light on the decrease in source confusion as the observation time is extended. As the time of observation is increased the improvement in the resolution of the power spectra (as observed in Fig. 3) of two or more sources can allow for separation of spectra that might overlap given a shorter time of observation.

C. Uncertainty ratios as a function of signal correlation

Figure 11 plots the median GMUR versus the signal correlation for a galactic draw when two binaries are present within $\delta f = f_m$ of each other. The plot shows that the GMURs increase faster than exponentially as the signal correlation increases. While a link between signal correlation and uncertainty ratios is to be expected, the superexponential nature of the relationship came as a surprise.

The rapid increase in the parameter uncertainties with signal correlation explains the results seen in Sec. VI A. As the time of observation is increased the magnitude of the correlation of the signals will be decreasing as $1/T_{\text{obs}}$ (seen in Fig. 9). This decrease in the signal correlation translates into the much faster decrease in the GMUR as a function of observation time (seen in Fig. 6).

Figs. 12 and 13 show the spreads for correlation and GMUR in the same data run. As can be seen in the log-linear scale of Fig. 13, the GMUR falls off exponentially from its most frequent value of 1.2.

While Fig. 12 shows the results for two correlated binaries, its results can be extended to multiple correlated binaries. For example, in the figure one can see that 87% of the pairs of binaries have correlation magnitudes $|\kappa| < 0.5$. Thus with N binaries the probability that there will be a pair of binaries with $|\kappa| > 0.5$ grows as $1 - 0.87^{[N(N-1)/2]}$. As binaries overlapping in frequency are expected to number from tens to tens of thousands, the probability of having high correlations is very close to 1.

D. Uncertainty ratios as a function of base frequency

Figure 14 shows how the parameter uncertainty ratios depend on base frequency. The plots are for all-sky and galactic draws with two binaries for 1 yr of observation. The base frequency f_{base} was varied between 0.01 and 10 mHz, while the frequency of the second binary was randomly chosen between f_{base} and $f_{\text{base}} + f_m$. The GMUR was found to be fairly constant below 1 mHz, followed by a rapid decrease at frequencies above 1 mHz. This behavior can be traced to the different Doppler shifts experienced by each source. The motion of LISA relative to a source located at (θ, ϕ) imparts a Doppler shift equal

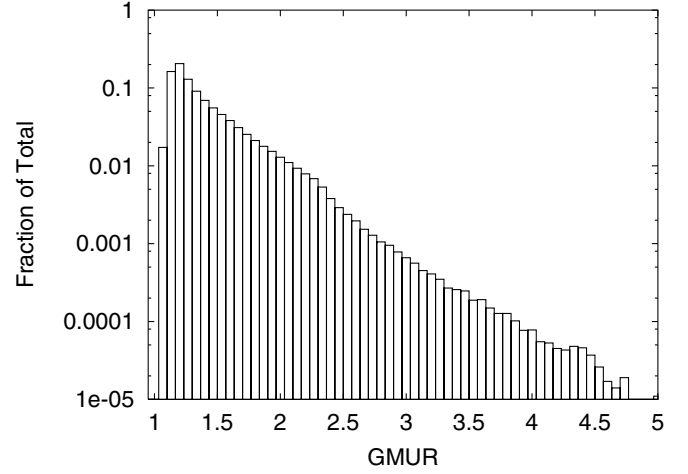


FIG. 13. A histogram of the GMUR of two binaries from a galactic draw with a base frequency of 1 mHz and 1 yr of observation of 10^6 pairs of sources within $1f_m$ of each other.

to

$$\delta f_D \simeq \pi \sin \theta \sin(2\pi f_m t - \phi) \left(\frac{f}{\text{mHz}} \right) f_m. \quad (16)$$

The magnitude of δf_D becomes comparable to the frequency resolution $\delta f = 1/T_{\text{obs}} = 1/\text{yr}$ for $f \sim 0.3$ mHz. Sources that are well separated in ecliptic azimuth ϕ will experience Doppler shifts that differ in sign, as LISA will be moving toward one source and away from the other. Thus, we expect that the degree of source confusion will depend on the azimuthal separation of the two sources. Our expectations are confirmed in Fig. 15, where the dependence of the GMUR on azimuthal separation is plotted for base frequencies of 0.1 and

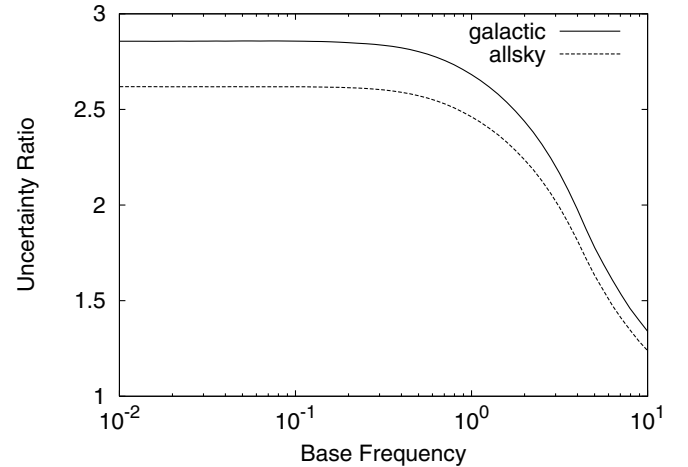


FIG. 14. Median GMUR plotted against base frequency of two binaries from all-sky and galactic draws with 1 yr of observation of 10^5 pairs of sources. The drop off in the median GMUR is due to the increasing Doppler shifts which separate the sources in frequency and thus decrease signal confusion (as seen in Fig. 10).

1 mHz. Unfortunately, most galactic sources are within $\sim 20^\circ$ degrees of each other in ecliptic azimuth, which helps explain the larger GMURs for the galactic distribution as compared to the all-sky distribution.

VII. INFORMATION THEORY PERSPECTIVE

There have been several attempts to understand LISA source confusion in the framework of information theory [13–15]. According to Shannon [16], the maximum amount of information that can be transmitted over a noisy channel with bandwidth B in a time T_{obs} is

$$I_S = BT_{\text{obs}} \log_2 \left(1 + \frac{P_h}{P_n} \right). \quad (17)$$

Here P_h and P_n are, respectively, the signal and noise power across the bandwidth. (Note: The SNR ratio is related to these quantities by $\text{SNR}^2 \approx BT_{\text{obs}} P_h / P_n$). As an example, a typical bright galactic source at 1 mHz with $P_h/P_n \sim 10$ can transmit at most $I_S \approx 70$ bits of information in 1 yr via the two independent LISA data channels S_I and S_{II} . In practice the actual information content will be somewhat less due to suboptimal encoding. It takes $\log_2(x/\Delta x)$ bits of information to store a number x to accuracy Δx , thus the total amount of information required to describe a monochromatic binary to a precision $\Delta \vec{\lambda}$ is

$$I_\Delta = \log_2 \left(\frac{f}{\Delta f} \right) + \log_2 \left(\frac{A}{\Delta A} \right) + \log_2 \left(\frac{\pi}{\Delta \theta} \right) + \log_2 \left(\frac{2\pi}{\Delta \phi} \right) \\ + \log_2 \left(\frac{\pi}{\Delta \psi} \right) + \log_2 \left(\frac{\pi}{\Delta t} \right) + \log_2 \left(\frac{2\pi}{\Delta \gamma} \right). \quad (18)$$

Using the results in Fig. 1 for a bright galactic source at 1 mHz with $P_h/P_n \sim 10$, we find that $I_\Delta \approx 45$, which

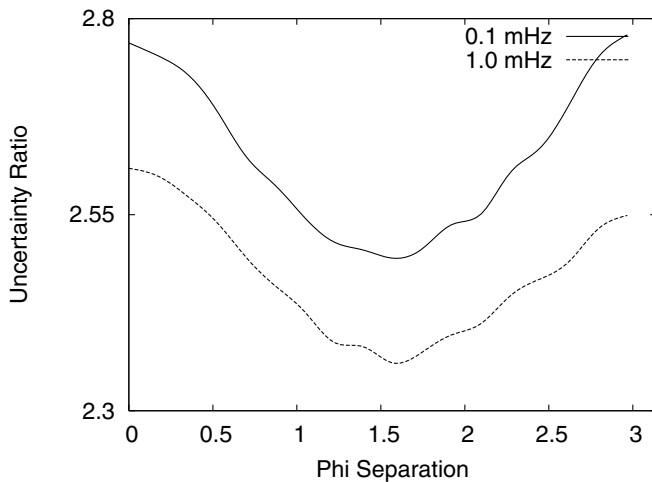


FIG. 15. Median GMUR plotted against azimuthal sky separation for two pairs of binaries from a galactic draw with 1 yr of observation with base frequencies of 0.1 and 1 mHz of 10^5 pairs of sources each.

indicates that the encoding, while suboptimal, is quite respectable.

One might hope that information theory could be used to predict some of the other results described in Sec. VI. Unfortunately, this proves not to be the case, for while information theory sets limits on how well one might do, it sets no limits on how poorly. The scaling of the GMUR as a function of the number of sources is a good example. The information needed to localize N galactic sources is equal to

$$I_\Delta(N) = \log_2 \left(\frac{V_{7N}}{\Delta V_{7N}} \right), \quad (19)$$

where ΔV_{7N} is given by (7) and $V_{7N} = V_7^N$ is the volume of the $7N$ dimensional parameter space. Requiring that $I_\Delta(N) < I_S(N)$ yields a lower bound on the geometric mean of the parameter uncertainties (GMU) of

$$\text{GMU} > \frac{V_7^7}{(1 + P_s/P_n)^{BT_{\text{obs}}/7N}}. \quad (20)$$

Consider first the case of N isolated binaries of similar brightness. The power ratio P_s/P_n will be independent of N , and the bandwidth will be the sum of the bandwidths of each signal, so B will grow linearly with N . Thus, Eq. (20) implies that for isolated binaries, the parameter uncertainties will be independent of the number of sources. This is indeed the case, as the Fisher information matrix is block diagonal for isolated sources. Now consider the case of N overlapping binaries sharing the same fixed bandwidth B . The power P_s will grow approximately linearly with N , leading to the prediction that the GMU must grow faster than $(1/N)^{(1/N)}$. The actual scaling seen in Figs. 7 and 8 tell a different story, with the GMUR increasing as $\sim N^N$. Thus, while information theory provides a lower bound on how quickly the parameter uncertainties must increase with the number of overlapping sources, the bound is too weak to be of any real use. The weakness of the bound is probably related to how poorly the information for multiple overlapping binaries is encoded.

VIII. DISCUSSION

We have found that source confusion will significantly impact LISA's ability to resolve individual galactic binaries. We found that source confusion affects parameter estimation fairly uniformly across the seven parameters that describe a galactic binary.

The two most significant findings were that source confusion grows exponentially with the number of correlated sources, and that source confusion decreases rapidly with time of observation.

Source confusion will be a significant problem in the frequency range between 0.01 and 3 mHz, where it is

estimated that there are upwards of 10^8 galactic binary systems. The decrease in the parameter uncertainties with time of observation is far greater than the usual $1/\sqrt{T_{\text{obs}}}$ decay that occurs when competing against stationary, Gaussian noise. The fast improvement is due to the $1/T_{\text{obs}}$ decrease in the source cross correlation, and the sensitive dependence of the parameter uncertainties on the degree of cross correlation.

Our findings suggest that earlier work that treated the galactic background as stationary, Gaussian noise should be revisited, and that every effort should be made to

extend the LISA mission lifetime beyond its nominal 3 yr duration.

This work was completed solely using optimal signal processing, solving for all sources simultaneously, rather than suboptimal signal processing, in which a source is solved individually while others are disregarded or treated as an effective noise. The results provided by suboptimal signal processing will be worse for estimation of the parameters. A different analysis would be needed to place a bound on how much of an effect such an approach would have.

-
- [1] P.L. Bender *et al.*, NASA/ESA Report No. MPQ 233 (1998).
 - [2] C. Cutler, Phys. Rev. D **57**, 07089 (1998).
 - [3] T. A. Moore and R. W. Hellings, Phys. Rev. D **65**, 062001 (2002).
 - [4] R. Takahashi and N. Seto, Astrophys. J. **575**, 1030 (2002).
 - [5] S. A. Hughes, Mon. Not. R. Astron. Soc. **331**, 805 (2002).
 - [6] N. Seto, Phys. Rev. D **66**, 122001 (2002).
 - [7] A. Vecchio, Phys. Rev. D **70**, 042001 (2004).
 - [8] L. Barack and C. Cutler, Phys. Rev. D **69**, 082005 (2004).
 - [9] D. Hils, P. L. Bender, and R. F. Webbink, Astrophys. J. **360**, 75 (1990).
 - [10] M. Tinto and J. W. Armstrong, Phys. Rev. D **59**, 102003 (1999).
 - [11] L. J. Rubbo, N. J. Cornish, and O. Poujade Phys. Rev. D **69**, 082003 (2004)
 - [12] C. Cutler and E. E. Flanagan, Phys. Rev. D **49**, 2658 (1994).
 - [13] N. J. Cornish, gr-qc/0304020.
 - [14] S. Phinney, "Proceedings of the Fourth International LISA Symposium, July, 2002."
 - [15] R. Hellings, "Proceedings of the International Conference on Gravitational Waves: Sources and Detectors, Casinica, 1996."
 - [16] C. E. Shannon, Bell Syst. Tech. J., **27**, 379 (1948). **27**, 623, (1948).